JOURNAL OF GEOPHYSICAL RESEARCH, VOL. 105, NO. E6, PAGES 15,061–15,071, JUNE 25, 2000

Noble gas abundance and isotope ratios in the atmosphere of Jupiter from the Galileo Probe Mass Spectrometer

P. R. Mahaffy,[1] H. B. Niemann,[1] A. Alpert,[2] S. K.Atreya,[3] J. Demick,[4] T. M. Donahue,[3] D. N. Harpold,[1] and T. C. Owen[5]

Abstract. The Galileo Probe Mass Spectrometer provided the first data on the noble gas mixing and isotope ratios in the Jovian atmosphere. These measurements and the comparison with solar values constrain models of Jupiter's formation. Significant refinements to the initially reported abundances of argon, krypton, and xenon have been enabled through post-encounter laboratory calibrations using a refurbished engineering unit mass spectrometer nearly identical to the flight unit. The abundances relative to hydrogen for argon, krypton, and xenon are respectively 2.5 ± 0.5, 2.7 ± 0.5, and 2.6 ± 0.5 times the solar ratios. The mixing ratios of He and Ne found in these studies are consistent with previously reported values of 0.8 and 0.1 times solar respectively. The Jovian $^{36}Ar/^{38}Ar$ ratio is 5.6 ± 0.25 and the $^{20}Ne/^{22}Ne$ ratio is 13 ± 2, consistent with the solar values of 5.77 and 13.81, respectively, that are derived from lunar mineral grain analysis. The distribution of xenon isotopes at Jupiter also resembles the solar distribution.

1. Introduction

The abundance distribution of the various elements in the atmosphere of Jupiter provides insight into the mechanism of the formation of this planet. Several of these values have been established by the in situ measurements from the Galileo Probe Mass Spectrometer (GPMS) [*Niemann et al.*, 1992]. The ratio of argon to hydrogen at Jupiter relative to this same ratio on the Sun, for example, can be compared to this ratio for the heavier noble gases, krypton and xenon, and more abundant elements, such as C, N, O, and S. These data together with laboratory studies [*Bar-Nun et al.*, 1988] of the relative extent of noble gas trapping in ices formed at different temperatures provides information on the formation temperature of the grains that are assumed to have generated planetesimals early in the history of the solar system. Current models of solar nebular evolution postulate that the giant planets formed by accretion of the equivalent of several earth masses of planetesimals [*Owen and Bar-Nun*, 1995; *Mizuno*, 1980; *Pollack et al.*, 1986; *Pollack and Bodenheimer*, 1989] in the initial stages of their formation until a large enough mass was achieved that direct gravitational capture of the gases not trapped in planetesimals (H_2, He, and Ne) occurred.

Owen et al. [1999] have recently suggested that the greater than solar ratios of Ar/H and N/H derived from these GPMS data and from analysis of the probe radio signal [*Folkner et al.*, 1998], respectively, point toward very cold (<30 K) formation temperatures of the planetesimals that formed this planet. It is proposed that these planetesimals therefore may not be identical to Oort cloud comets that evidently are depleted in N [*Krankowsky*, 1991; *Wyckoff et al.*, 1991], presumably due to inefficient trapping of N_2 at the 55 K formation temperature of these bodies.

Fractionation of the different noble gases during the evolution of the atmosphere of a planet can be used to test theories of various mechanisms of atmospheric loss from the terrestrial planets [*Pepin*, 1991]. The ratios found in the Sun and in the giant planets are expected to represent the values for these ratios in the protosolar nebula. Differences in the noble gas ratios between the Sun and Jupiter, however, would suggest a fractionation process in the formation of the grains and planetesimals that formed Jupiter.

This work describes the derivation of the noble gas mixing ratios from the GPMS data. Refinements are also given to noble gas isotope ratios previously reported [*Niemann et al.*, 1998, 1996]. These results were enabled by laboratory calibrations of the engineering unit (EU) GPMS. This unit was refurbished to make its performance as identical as possible to the flight unit (FU). The heavy noble gases, krypton and xenon, were detected in enrichment cell experiments involving trapping on a high surface area adsorbant. The EU experiments duplicated the variation of pressure with time encountered by the probe during its descent and the temporal variation of the temperature of the enrichment cells during the adsorption of these trace species. The more limited set of FU calibrations carried out in 1985 on the FU enabled a cross-check on the validity of the extrapolation of this calibration between the two instruments.

Extraction of the Jovian noble gas isotope ratios from the GPMS data requires a detailed consideration of instrumental effects. For example, the use of a highly miniaturized ion pump system operating throughout the descent from 0.4 to 22 bar ambient Jupiter pressure gave rise to a bias in the noble gas isotope ratios obtained for a portion of these measurements. The EU descent simulations allow these effects to be further quantified and the instrument pressure regimes established from which these ratios are most reliably obtained.

[2]Department of Planetary Sciences, University of Arizona, Tucson

[1]Laboratory for Atmospheres, Goddard Space Flight Center, Greenbelt, Maryland

[3]Department of Atmospheric, Oceanic and Space Sciences, University of Michigan, Ann Arbor

[4]Department of Engineering, Auburn University, Auburn

[5]Institute for Astronomy, University of Hawaii, Honolulu

Paper number 1999JE001224
0148-0227/00/1999JE001224$09.00

Section 2 of this paper describes the experimental aspects of the FU and EU mass spectrometer experiments and methods for the derivation of the abundances and isotope ratios. The noble gas signals over the course of the descent are shown in section 3; the mixing ratios of ^{4}He, ^{20}Ne, and ^{36}Ar discussed in section 4; the mixing ratios of krypton and xenon are discussed in section 5; the ^{20}Ne/^{22}Ne and ^{36}Ar/^{38}Ar ratios are discussed in section 6; the krypton and xenon isotope ratios are discussed in Section 7, and a summary discussion is given in section 8.

2. Experimental Aspects

2.1 The GPMS FU and the Descent Experiment

A detailed description of the GPMS [*Niemann et al.*, 1992] and a detailed discussion of the instrument sequencing during the descent [*Niemann et al.*, 1998] have been given and will be only briefly summarized here. A quadrupole mass spectrometer with a mass range of 1-150 dalton was employed that used redundant hot filament electron guns and had a dynamic range > 7 orders of magnitude. The mass spectrometer used a pulse-counting ion detector. A fixed detector integration period (IP) of 0.5 s was employed at each selected mass value, and the counts at 6863 IPs were measured over the course of the probe descent from 0.40 to 21.25 bar before signal from the GPMS and the probe ended. An ion signal at the detector near or above its saturation level (for example, at 4 amu from ^{4}He near the end of the descent) could switch the instrument into a reduced sensitivity mode for a single integration period. For convenience, the IPs during the course of the probe descent are labeled sequentially and designated as step numbers 1 to 6863. Programming of the masses used during the descent sequence was done during the instrument design and calibration.

Two separate gas manifolds were used at different times during the descent, each activated by pyrotechnic removal of inlet and outlet caps that allowed Jovian atmosphere to flow through the previously evacuated gas transfer lines of the instrument. This inlet and gas processing system allowed atmospheric gas to be sampled either directly into the ion source of the mass spectrometer through glass capillary pressure reduction leaks or after processing in one of two enrichment systems. The two direct glass capillary array leaks designated DL1 and DL2 were sized with a gas conductance appropriate for the pressure range expected during their use. The capillary array DL2 used in the final stage of the experiment beamed gas directly through the electron beam in the ion source of the mass spectrometer. Gas molecules passing through DL1, on the other hand, encountered several wall collisions en route to the ionization region because of the presence of valves in this line between the ion source and DL1. These redundant valves served to shut off the gas flow from the first inlet manifold just before the break off caps that activated the second inlet system were released. The enrichment system incorporated high surface area adsorbants through which atmospheric gas was pumped into a chemical getter. The getter removed chemically active gases, such as the major atmospheric species H_2. Subsequent thermal release of the gases adsorbed on the enrichment cell increased the detection threshold for trace species such as the heavy noble gases. The direct leaks DL1 and DL2 operated during the descent over the pressure ranges 0.508-3.78 bar (DL1, steps 83-1810), 8.59–12.08 bar (DL2a, steps 3482–4441), and 15.66–21.95 bar (DL2b, steps 5331–6863). The two enrichment cell experiments sampled gas from two atmospheric regions, 0.89 bar to 2.85 bar (steps 1340 to1695) and, subsequently, from the second inlet system from 8.89 bar to 9.56 bar (steps 3567 to 3756). The loading of the enrichment cells occurred concurrently with the direct sampling.

2.2 EU Calibration System

A schematic diagram of the gas flow paths in the laboratory system used to calibrate the EU is shown in Figure 1. Many elements of this calibration system were also used for calibrations of the FU prior to delivery of this instrument in 1985. The components enclosed within the upper (dotted line) box in Figure 1 are nearly identical in the EU and the FU. The pyrotechnically actuated inlet and outlet metal/ceramic breakoffs used in the FU to allow Jovian gas to flow through the gas processing lines of the instrument are replaced with valves in the EU. The EU can be configured to employ a pumping system nearly identical to that of the FU. This pumping system consists of a miniaturized ion pump and getter pumps. In addition, an oil-free turbomolecular pump (TP) based ultrahigh vacuum system is used for bakeout and vacuum processing of the EU. The locations of the valved lines to the turbomolecular pumped chamber are shown in Figure 1. Background pressures in this chamber are typically 1 x 10^{-11} mbar after bakeout. The conductance of the EU leaks DL2, L3, and L4 were within a few percent of the FU leaks. However, leak DL1 in the EU had a higher conductance by a factor of ~2 than the FU.

The components enclosed within the lower (dotted line) box in Figure 1 are specific to the calibration system and served to prepare gas mixtures resembling the Jovian atmosphere. The circulating system operates in the pressure range 0-23 bar and mixes the gases introduced into the manifold. Capacitance diaphragm (Validyne) pressure gauges PG1 and PG2 allow inlet pressures in the range 0.001-23 bar to be measured. The expansion volume is ~ 20 times the volume of the gas manifold. Through repeated cycles of gas expansion and then pumping and purging (to insure the complete removal of gas from this chamber) of the expansion volume, gas mixtures can be prepared with gas partial pressures well below the sensitivity threshold of the inlet pressure gauges. Typically, mixtures representative of the Jovian atmosphere in mixing ratios of both major and minor species were prepared containing up to 11 different gases. For example, for the noble gas calibrations described, the gas mixture typically consisted of at least H_2, He, Ne, Ar, Kr, Xe, CH_4, NH_3, H_2O, C_2H_4, and C_3H_8, all in approximately their Jovian mixing ratios.

The EU mass spectrometer analyzer, detector, ion source, and gas inlet system were a close copy of the FU. The GPMS quadrupole analyzer employed a dual fixed frequency RF system. A particular mass was selected for transmission through the quadrupole by setting the amplitude of the RF voltage and a DC voltage derived from the RF to allow only ions of a particular mass to charge ratio to transmit through the analyzer. The EU employed a flight-spare RF board in order to duplicate the behavior of the FU mass analyzer as closely as possible. The digital control circuits for the EU calibrations used a programmable Computer Automated Acquisition and Control (CAMAC) driven interface to allow complete flexibility in the selection of sequences of mass values and integration times. The CAMAC system also controlled the power supplies that supplied voltages to the ion and electron lenses and the detector system.

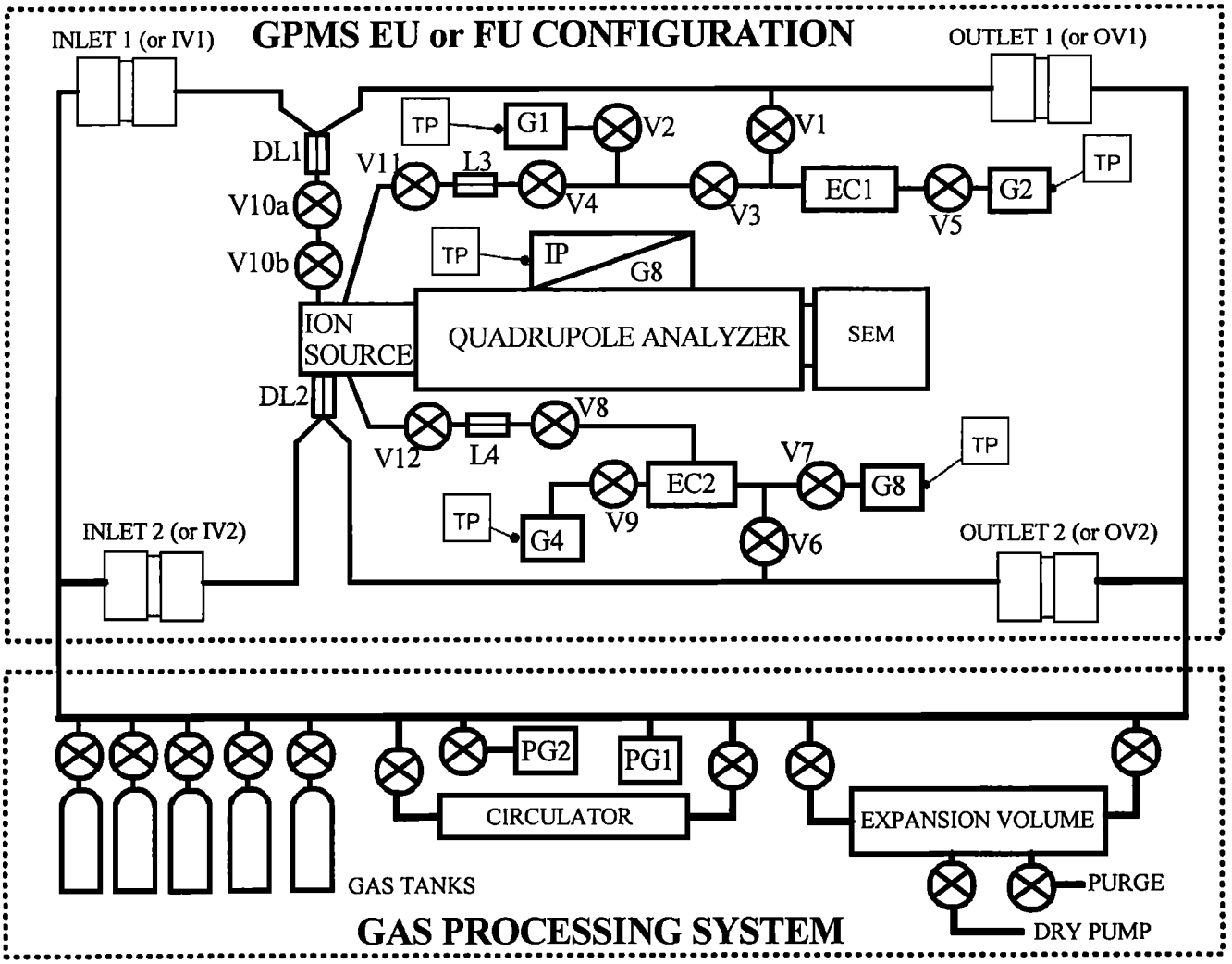

Figure 1. A diagram of the gas flow paths in the Galileo Probe Mass Spectrometer engineering unit or flight unit and the calibration system manifold showing valves (V), pressure gauges (PG), secondary electron multiplier (SEM), lines to the turbomolecular pump (TP), getters (G), the ion pump (IP), capillary leaks (DL or L), and enrichment cells (EC).

These voltages were set very close to the values used in the FU with small adjustments necessary to account for the small mechanical differences between the two systems. Lens voltages that were mass dependent in the FU were programmed with the identical function in the EU runs. High-resolution scans were carried out with the EU and compared with the one eighth amu resolution scans obtained from the FU during the descent. The EU RF tuning parameters that change the slope and intercept of the DC voltage as a function of mass were then set to give similar peak shapes as the FU scans. Similarly, the gain of the FU pulse-counting detector had been measured prior to launch as a function of detector voltage. The gain response of the EU detector obtained from the same detector batch was similarly characterized. When the EU detector response was found to deviate significantly from that of the FU, the detector was replaced.

As described by *Niemann et al.* [1998], ^4He, H_2, or one of the CH_4 fragments at 13 or 14 amu were used as a reference to establish the mixing ratio of other atmospheric species. In this case a calibration constant $C_i = (n_i/n_r)/([i]/[r])$ is first derived from calibration data. Here i designates the species of interest and r the reference species. Also, $[i]$ and $[r]$ designate the counts per integration period from species i or r at the mass used for calibration after all other contributions to this mass from backgrounds or other species have been subtracted. Here, n_i and n_r are the volume mixing ratios of the two species. C_i derived from FU or EU calibration data is then multiplied by the count ratios $([j]/[r])_j$ to obtain $(n_i/n_r)_j$ where the subscript j refers to the Probe GPMS data and derived Jovian mixing ratios. Absolute count rates are alternately used to calibrate the FU from the EU data. This is necessary for some of the data from the enrichment cells where the detector signal at the masses for ^4He or CH_4 fragments could be saturated.

Since the mixing ratios of krypton and xenon were too low for a direct leak determination, all data for these gases were obtained from the gas released during the enrichment cell experiments. The ratio of krypton to xenon trapped on these cells was a function of the enrichment cell temperature at the time of adsorption.

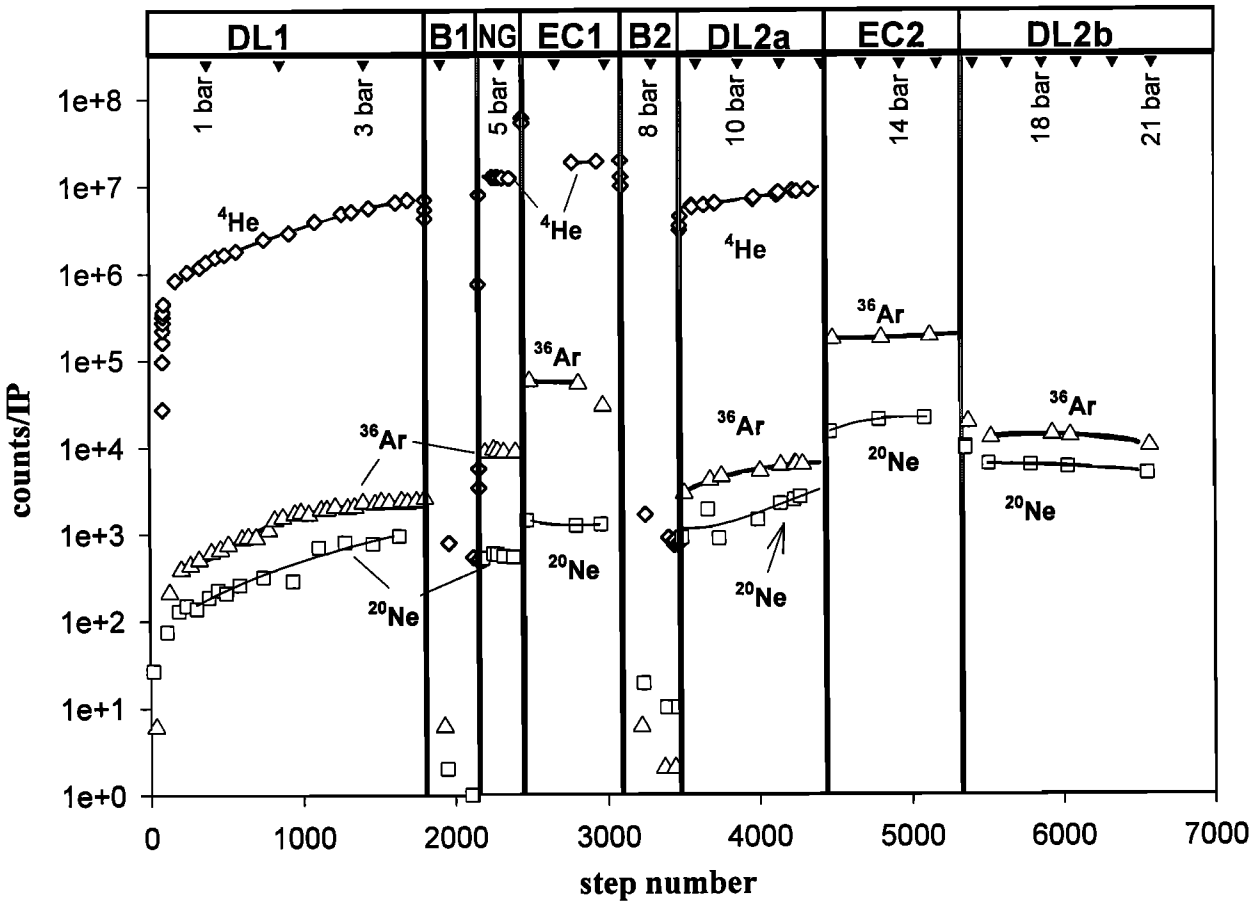

Figure 2. The signal from selected isotopes of the noble gases He, Ne, and Ar are shown over the 1 hour course of the descent. The symbols are the data points, and the lines show a polynomial fit within each measurement sequence. The measurement regions from left to right are direct leak 1 (DL1), the first background (B1), the noble gas experiment (NG), the first enrichment cell (EC1), the second background (B2), the first part of the direct leak 2 (DL2a), enrichment cell 2 (DL2), and the second part of the direct leak 2 (DL2b).

Stronger than expected thermal coupling of the Jovian atmosphere to the Probe instrument-mounting platform resulted in temperature variations in the enrichment cells during the noble gas trapping experiment. For example, it is estimated from the housekeeping data that the temperature of EC1 was approximately -5°C at the time this cell was exposed to the Jovian atmosphere and reached a minimum temperature of approximately −15°C during the adsorption. Similarly, the temperature of EC2 increased from 10°C to 15°C over the course of the gas adsorption. The EU calibration runs duplicated the temperature and pressure profile encountered by the cells of the FU. Getter G4 encountered a pressure of 9.56 bar at the end of its adsorption period. At this pressure the getter rapidly saturates with hydrogen. In order to duplicate the conditions encountered during the encounter, this getter was changed out after each EU run that duplicated this enrichment cell experiment. All other pumps were also replaced on a periodic basis.

3. Signal from Selected Noble Gas Isotopes Over the Course of the Descent

Figure 2 shows the counts per integration period (of 0.5 s) over the entire Probe descent for ^{4}He, ^{20}Ne, and ^{36}Ar. Figure 3 is a similar plot for ^{84}Kr and ^{129}Xe. All data points are shown for these noble gas isotopes except for those points at 4 amu where the mass spectrometer was switched into the low sensitivity mode. The raw data have been corrected for detector dead time effects following a procedure that has previously been described [*Niemann et al.*, 1998]. Full mass spectra in each of the direct leaks and in each of the enrichment cells are shown in Figures 4 and 5. Krypton and xenon appear first in the enrichment cell experiments, and the signal in DL2a and DL2b from these species is primarily the background signal from these gases previously produced in the enrichment cells.

4. Mixing Ratios of ^{4}He, ^{20}Ne, and ^{36}Ar

These mixing ratios are derived from the DL1 and DL2 data. Calibration constants were obtained for these species in EU runs using a gas mixture that very closely matched the Jovian mixing ratios as described above. These calibrations confirmed the previously reported mixing ratio for ^{4}He of 0.157 relative to H_2 (or 0.8 times the solar value). Similarly, a mixing ratio for ^{20}Ne was found of 2.3×10^{-5} (or ~0.1 times solar), consistent with the previously reported value. However, the mixing ratio for ^{36}Ar previously reported as ≤1.7 times the solar value [*Anders and*

Grevesse, 1989] relative to H_2 was found to be somewhat greater with these additional EU experiments. The previously reported value [*Niemann et al.*, 1998] was based on a limited set of 1985 FU calibration runs. In these laboratory calibration runs, there was a substantial drift in the [4]/[2] ratio in different mass scans within the data set, suggesting a possible incomplete mixing of the gases in the inlet lines. When several EU runs are averaged together with these results, we obtain a mixing ratio for argon that is 2.5 ± 0.5 times solar. This average is heavily weighted toward the EU calibration results in view of the issues with the more limited set of FU calibration data described. The mixing ratio of $^{36}Ar/H_2$ from these calibrations is 15×10^{-6}.

Figure 6 shows the ratio in the FU Jupiter data to [4] of [2], [20], and [36] used to derive these mixing ratios. The count rates [2], [4], [20], and [36] are dominated by contributions from H_2, ^4He, ^{20}Ne, and ^{36}Ar, respectively. The small contribution from Ar^{++} to [20] has been removed to illustrate the $(^{20}Ne)/(^4He)$ count ratio. The absolute [36] counts in the EU runs and ratios to other species, such as H_2 or CH_4, are also consistent with the Ar mixing ratio calculated using ^4He as a reference. The scatter in the ^{36}Ar and ^{20}Ne ratios is generally larger than that expected from the detector-counting statistics and is attributed to variations in ion pump efficiency with pressure and to ion pump regurgitation effects where previously pumped gas is suddenly released, producing a short pressure burst in the pump that can propagate back into the ionization region. The calibration constants are generally not identical in DL1 and DL2 owing to the different geometry of gas introduction into the ionization region. This is particularly evident when comparing the [2]/[4] ratio in the two regions. Here H_2 is pumped primarily by the GPMS chemical getter pumping system, while He is only pumped by the ion pump. Small variations in these pumping speeds with pressure produce the small variation in this ratio near the high-pressure end of the DL2 region. The [2]/[4] ratio in the DL1 region is essentially constant over a wide pressure range. The [36]/[4] ratio is not shown for the DL2b region since [4] partially saturates the detector at these high ^4He ion source densities. However, the ratio of [36] to [13] (from a methane fragment CH^+ that does not saturate the detector) is nearly constant across the DL2a and DL2b regions.

5. Mixing Ratio of Krypton and Xenon

The mixing ratios of krypton and xenon were derived entirely from EC1 and EC2 data obtained during the descent compared with postencounter EU calibrations on both enrichment cells. The krypton value is 2.7 ± 0.5 times the solar value of 3.4×10^{-9} relative to H_2 [*Anders and Grevesse*, 1989] and was derived from the most abundant isotope, ^{84}Kr. Although this analysis assumes the remaining Kr isotopes are present in their solar ratios, the reported value of 2.7 times solar changes by, at most, 0.1 if this assumption is not employed. For the xenon

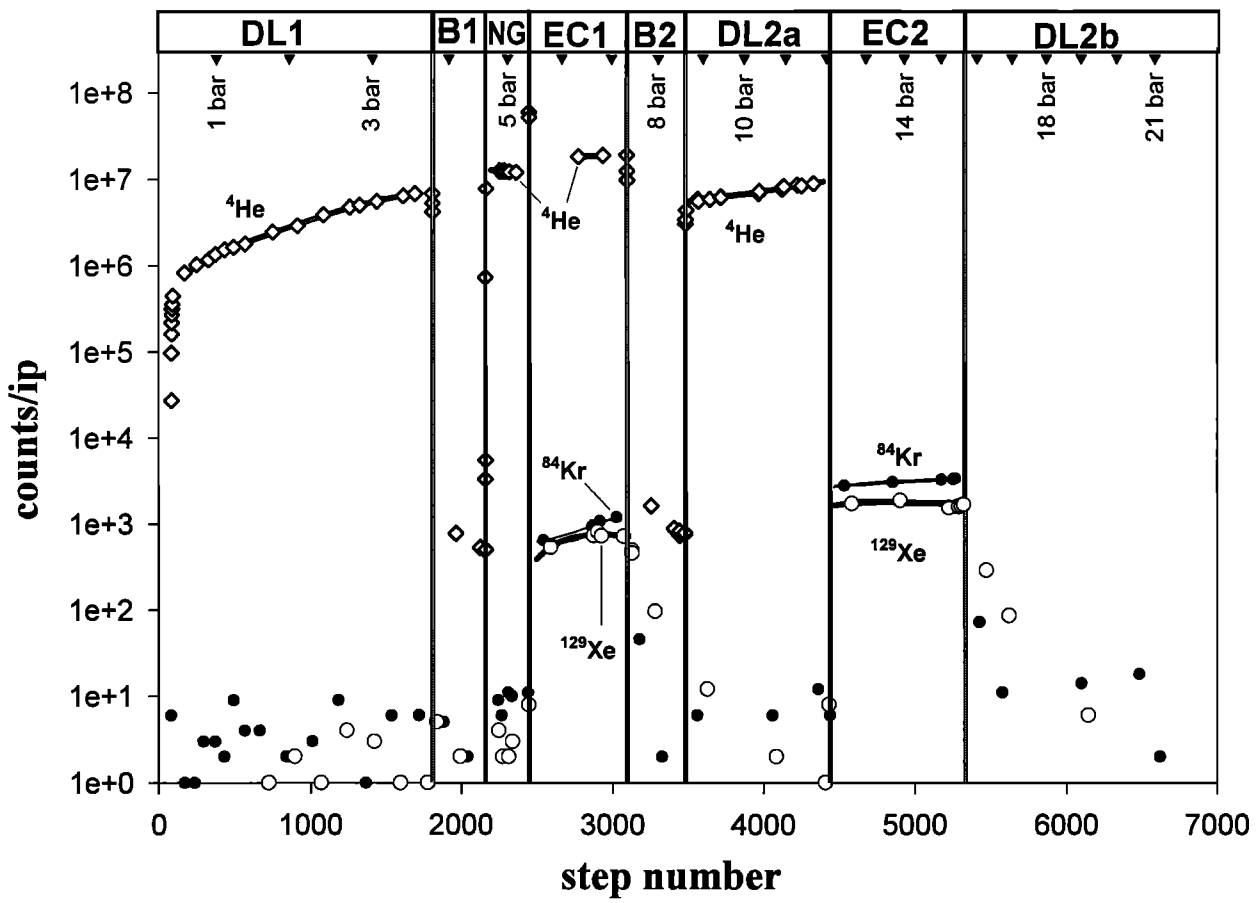

Figure 3. The signals from selected isotopes of the noble gases He, Kr, and Xe. The regions are labeled as in Figure 2.

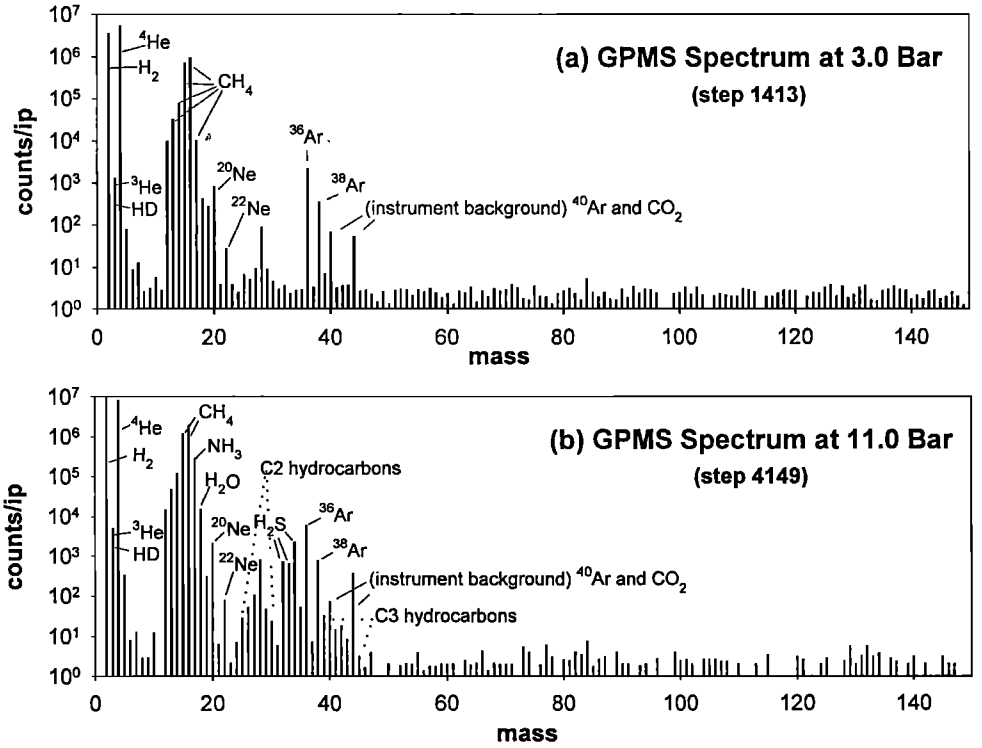

Figure 4. Full mass spectra from each of the direct leaks shown at Jovian pressures of (a) 3.0 bar and (b) 11.0 bar. The polynomial fit to the signal at each mass is used at the selected pressure to obtain these spectra. The heavy noble gases, krypton and xenon, are below the sensitivity threshold of the instrument in the direct leak mode.

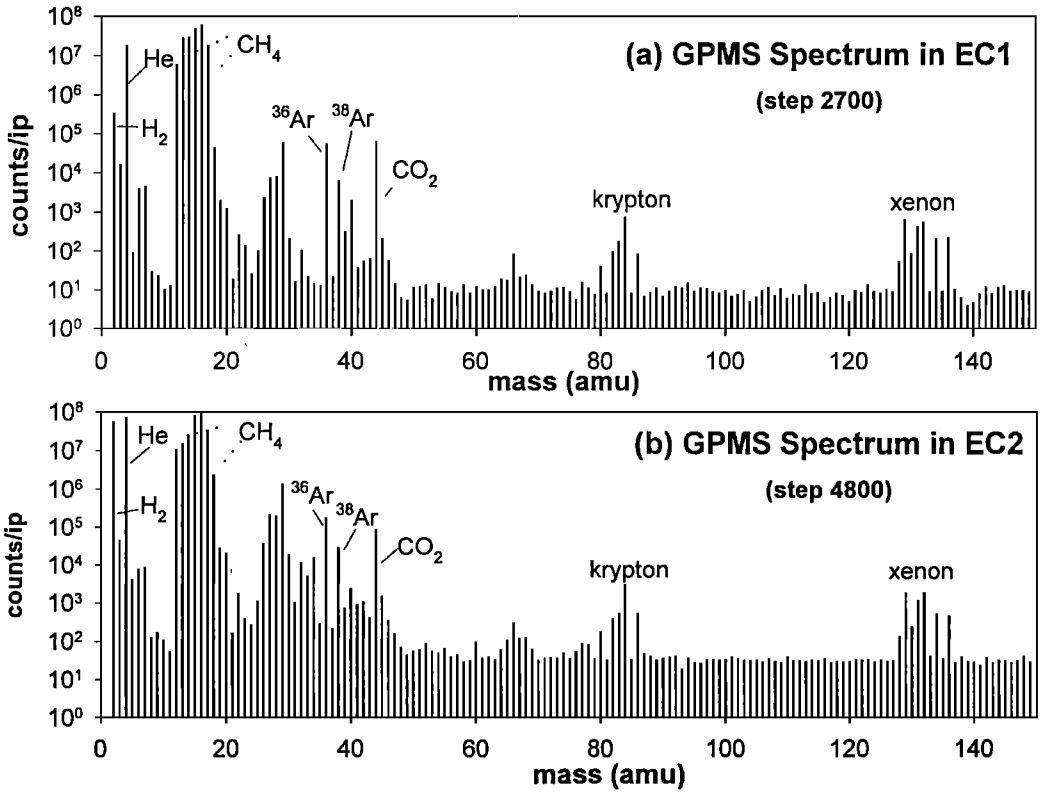

Figure 5. Full mass spectra from (a) enrichment cell EC1 and (b) enrichment cell EC2. The krypton and xenon are thermally desorbed from the chemical traps at the point these spectra were obtained.

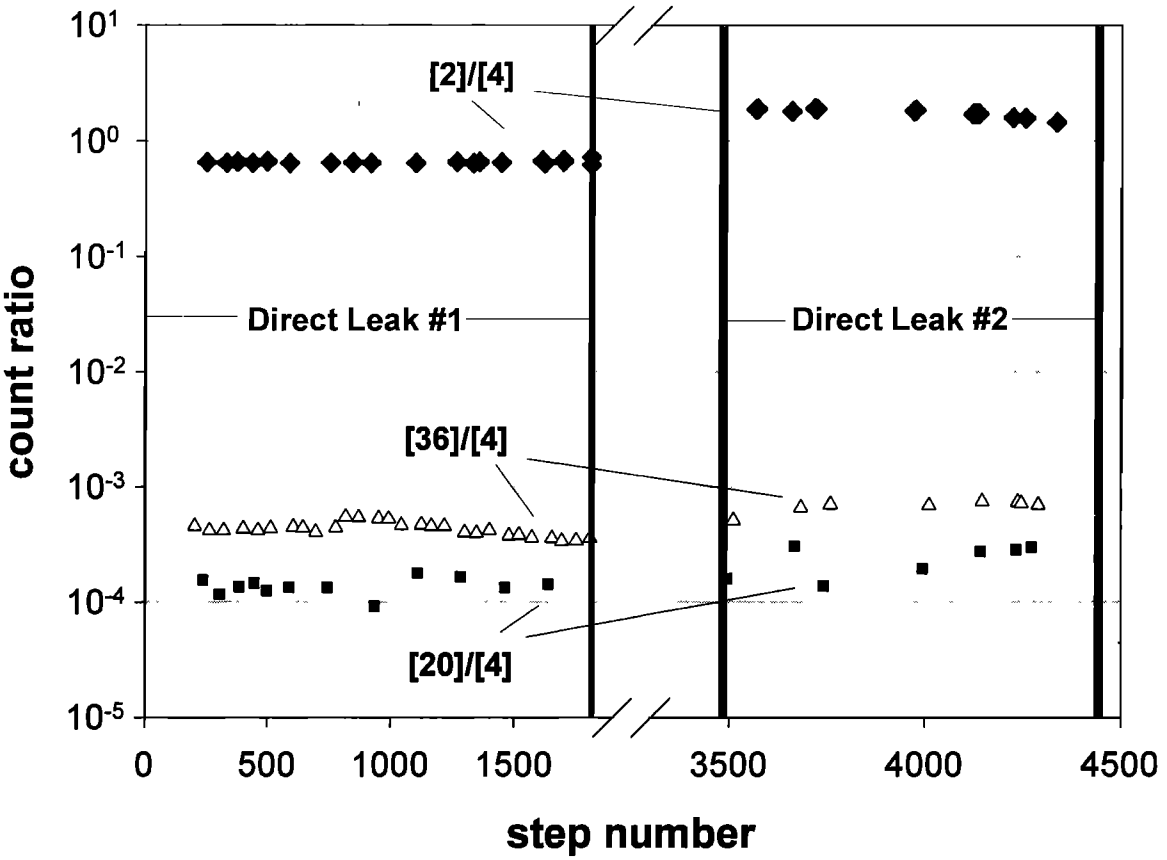

Figure 6. Count ratios to ^{4}He of [2]/[4], [20]/[4], and [36]/[4] shown for the GPMS Jupiter DL1 and DL2 regions where the H_2, ^{20}Ne, and ^{36}Ar mixing ratios were obtained. The [4] value at each step is calculated from the polynomial fit shown in Figure 2. A small contribution to [20] from $^{40}Ar^{++}$ has been removed.

mixing ratio determination the sum of all the major xenon isotopes at 128, 129, 130, 131, 132, 134, and 136 amu was used in the analysis. The ^{124}Xe and ^{126}Xe signals were below the detection threshold of the enrichment cell experiment. The xenon mixing ratio was found to be (2.6 ± 0.5) times the solar value of 3.4×10^{-10} relative to H_2 [*Anders and Grevesse*, 1989]. The EU unit had been refurbished some time after the Jupiter encounter to make the enrichment cell capillary leaks as close as possible in conductance to those in the flight unit. In several experiments, the four tubes that connected the enrichment cell portion of the EU to the turbomolecular pumped vacuum chamber were pinched off after getter activation in an identical manner to the FU. The duplication of enrichment system volumes, the preparation of a gas mixture that closely resembled the mixing ratio in the atmosphere encountered by the GPMS FU, its introduction to the enrichment cell system in the time/pressure sequence encountered by the FU, and the control of the enrichment cell temperatures to match those encountered during the descent forced the EU calibration experiments to approximate the FU conditions very closely.

6. Light Noble Gas Isotope Ratios

The ^{3}He/^{4}He Jupiter isotope ratio of $(1.66 \pm 0.05) \times 10^{-4}$ has previously been reported [*Mahaffy et al.*, 1998]. The Jovian ^{36}Ar/^{38}Ar ratio is 5.6 ± 0.25 and the ^{20}Ne/^{22}Ne ratio is 13 ± 2. Figure 7 gives the [36]/[38] ratio in the DL1, NG, EC1, DL2a, EC2, and DL2b regions. No other species or fragments have been identified that are contributing significantly to the [38] or [36] signals. However, it is evident that the [36]/[38] count ratio does not approach a constant value until a count rate of several hundred per second is achieved for both isotopes in the very last part of DL2a, EC2, and DL2b. Noble gases are well known to be difficult to pump because of their chemical inertness, and the observed variation in the [36]/[38] ratio at low density for these species is believed to be due to instrumental effects, primarily to isotopic fractionation effects on the clean ion pump cathode surfaces. Different efficiency in burial and rerelease of a portion of the pumped gas for the two isotopes at the initial very low partial pressures shows up as a variation in the [36]/[38] ratio until a steady state pumping condition is achieved at higher ion pump pressures. Here there is likely a more efficient removal of these isotopes with a higher fraction of multiply ionized species created in the pump. The EC2 and the DL2b regions are thus regarded as the best regions from which to obtain ^{36}Ar/^{38}Ar isotope ratios. At these higher ion source pressures the pumping speed for argon and neon becomes more constant, as is evidenced by examination of ratios of these signals to a methane fragment, such as $^{12}CH_2^+$, the dominate signal at 14 amu. This interpretation is supported by EU descent simulation runs where similar variations in the ^{20}Ne/^{22}Ne ratio are observed over the first part of the sequence on a new ion pump but the ratio approaches the terrestrial value near the high-pressure end of the sequence.

The ^{20}Ne/^{22}Ne ratio given is obtained from the DL2b region since in the DL2a region the [22] signal is still low at < 100 counts per integration period and in the EC2 region, there are

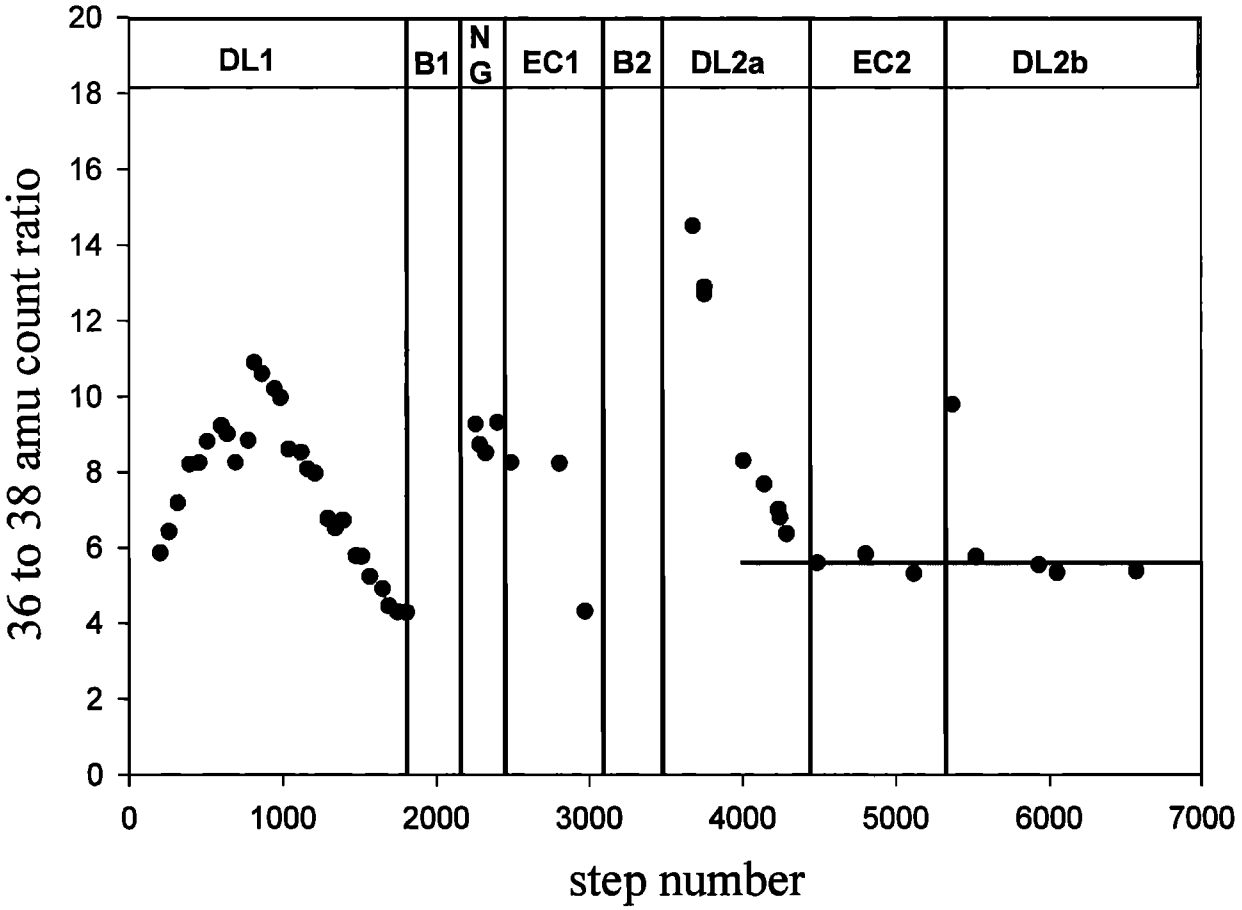

Figure 7. The [36] to [38] ratio in the DL1, NG, EC1, DL2a, EC2, and DL2b regions.

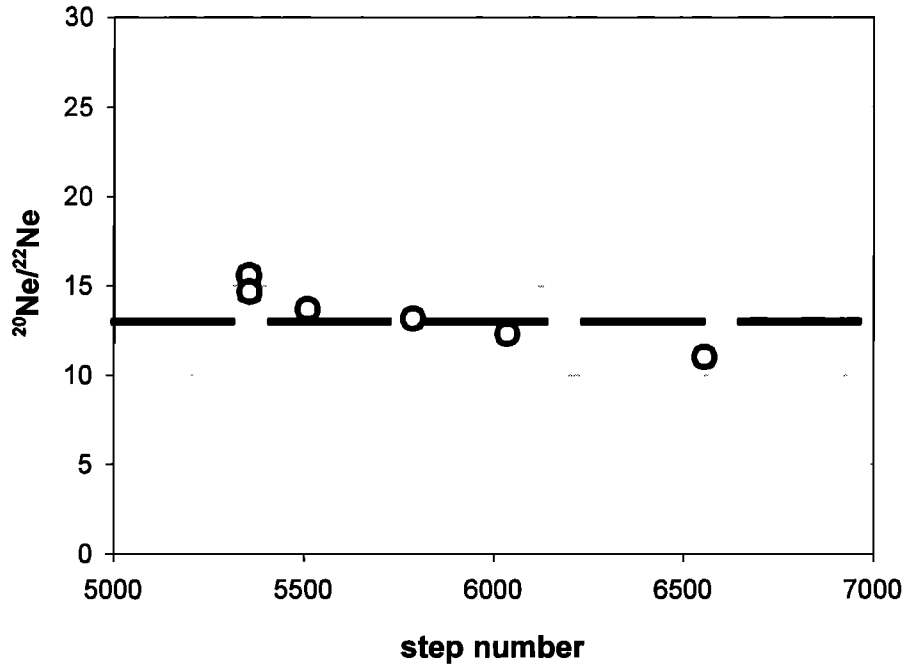

Figure 8. The [20] to [22] count ratio in the DL2b region after contributions to [20] from $^{40}Ar^{++}$ and $H_2{}^{18}O$ and contributions to [22] from $CO_2{}^{++}$ have been subtracted.

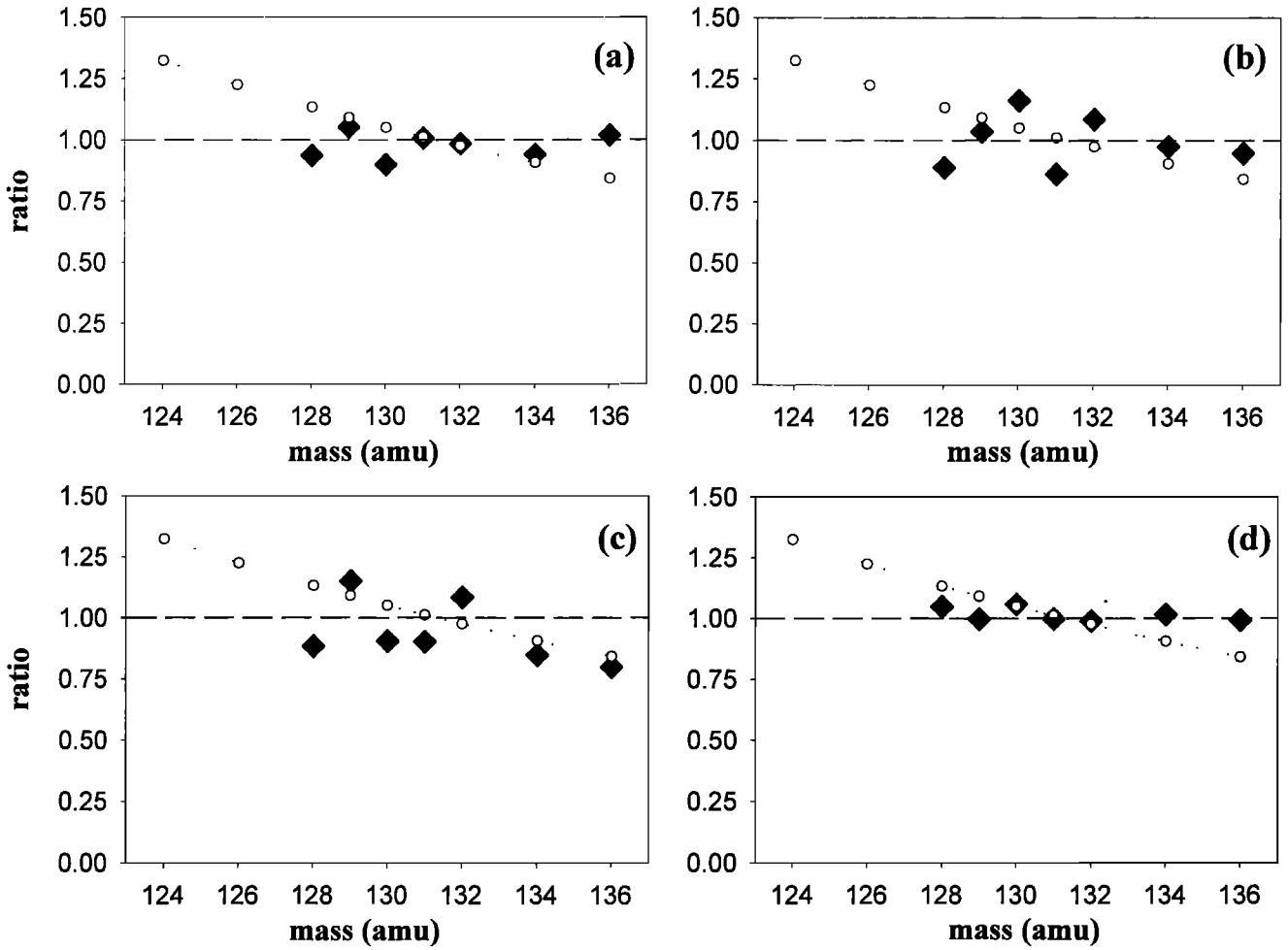

Figure 9. The ratio of Jovian xenon abundance to the nonradiogenic terrestrial xenon. The open circles show for comparison the assumed solar U-Xe [*Pepin*, 1991] for (a) the EC1 data, (b) the exponential decay of the background signal after the valve to the EC1 region was closed, and (c) the EC2 region. (d) for comparison, the ratio to terrestrial xenon obtained when this experiment was carried out in the laboratory using the EU.

substantial contributions to the [20] and [22] counts from other species, as is evident from the EC2 spectrum shown in Figure 5. The [20]/[22] ratio in the DL2b region is shown in Figure 8 after contributions to [20] from $^{40}Ar^{++}$ and $H_2{}^{18}O$ have been subtracted as well as contributions to [22] from $CO_2{}^{++}$. The contributions of doubly charged species were established through EU studies, and a contribution to [20] was calculated assuming a terrestrial $^{18}O/^{16}O$ ratio. A 50% variation in the latter ratio only changes the calculated $^{20}Ne/^{22}Ne$ ratio by 5%. However, there are evidently still some pump effects on this ratio or residual contributions from other species to one or both of these masses, as evidenced by the drift in this ratio through this region. The large error bars reflect the uncertainty in this ratio.

7. Isotope Ratios of Krypton and Xenon

The xenon composition was obtained by the following procedure. The 1985 FU calibration data established that the final tuning of the FU left a very small cross talk present in the mass range of the xenon isotopes from a higher mass to a lower mass peak of 0.0059 times the intensity of the higher mass signal. The first step in this analysis was to subtract this cross talk from the GPMS Jupiter data. An additional point by point correction applied to each isotope was derived from this FU 1985 calibration data. This correction accounted for fine structure on the peaks that was present at these high masses. This structure, combined with a small offset of the exact isotopic mass from that sampled, made this correction necessary. The average magnitude of this correction was 0.044 times the peak intensity. The ratio of the Jupiter xenon isotopic abundance derived from EC1 is shown in Figure 9a as a ratio to the nonradiogenic terrestrial xenon isotopic abundance [Pepin, 1991]. The assumed solar or "U-Xe" xenon given by Pepin [1991] is also shown in this plot. Five or six individual data points for each xenon isotope were obtained from the GPMS in the EC1 region. Since there was a small drift in this signal intensity during the EC1 measurement (likely due to small changes in the temperature of the enrichment cell), a polynomial fit was used for each isotope and 5 step values within this region selected to sum for each isotope to give the points used in the plot shown in Figure 9 (a). In Figure 9b the signal immediately after the EC1 valve to the mass spectrometer was closed is used to obtain a similar set of ratios. This decay for each isotope is fit well by an exponential as the gas is removed by the high-vacuum pumping system and the intensity at the step just after the valve was closed is used to obtain the ratios shown. In EC2 the mass spectrometer pressures are very high, and a considerable level of

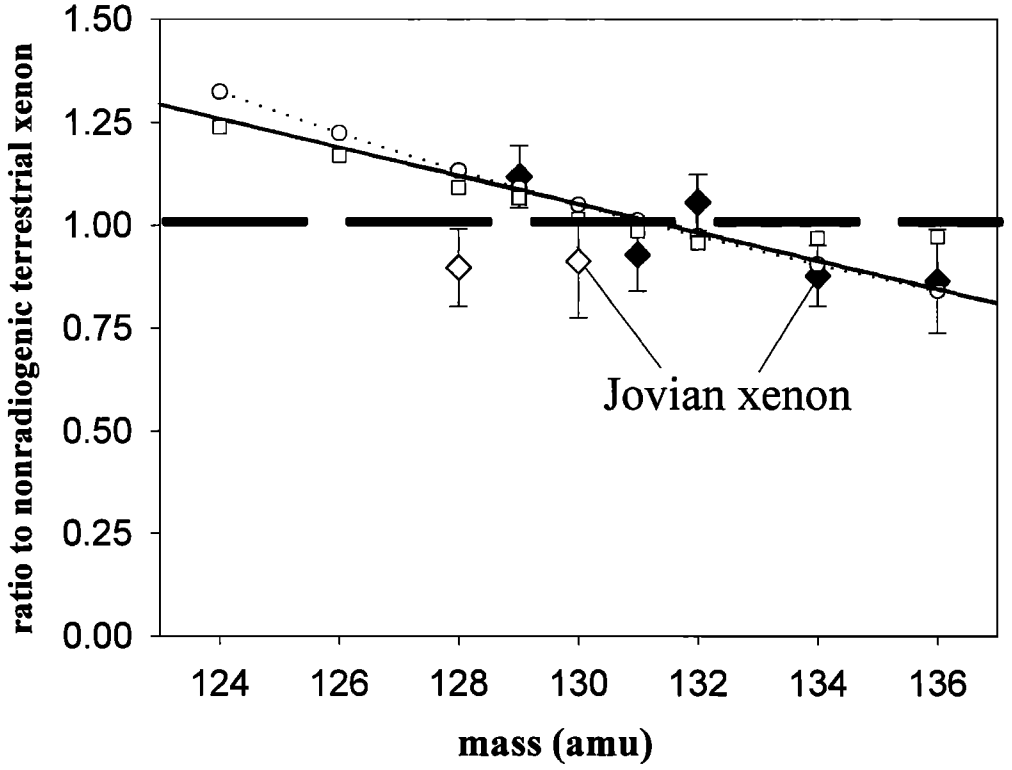

Figure 10. A count-weighted average of the three xenon composition results illustrated in Figure 9, together with the associated error bars for each isotope. For comparison, the assumed solar U-Xe values of *Pepin* [1991] (open circles and dotted line) and the values suggested by Pepin [1991] for CI chondrites (open squares) are shown. A linear regression line (solid) is drawn through the isotopes present at 5% or greater relative to the total xenon. Derivation of the error bars is described in the text. The isotope ratios used to generate this line are shown as solid diamonds, while the two minor isotope ratios are shown as open diamonds. The ^{124}Xe and ^{84}Xe isotopes were below the sensitivity limit of either enrichment cell.

ion neutral scattering in the quadrupole analyzer region is present as inferred from the significant mass independent background evident in Figure 5b. A similar xenon analysis as described for the EC1 region was carried out in EC2 and gave the data shown in Figure 9c. Figure 9d shows data from the EU obtained in laboratory studies with the ratio to terrestrial xenon to study possible instrument bias effects. These EU data were obtained under identical EC2 conditions of xenon loading and total instrument pressure. The point by point correction applied to the FU data was not used since high mass resolution scans allowed the peak maximum to be identified in this case. Figure 9d shows a nearly flat instrument response for the xenon isotopes with the largest scatter in the minor isotopes 128 and 130 as expected. Figure 10 shows a count-weighted average of the three FU data sets shown in Figure 9. The diamond symbols in this plot are the Jovian data, and a linear regression line is drawn through the major (> 5%) isotopes. This line falls close to the U-Xe line given by *Pepin* [1991]. The xenon isotopic distribution for CI chondrites [*Pepin*, 1991] is also shown in Figure 10 for comparison. It is evident that the tuning of the mass spectrometer in the region of the xenon isotopes did not measurably drift since the value of the cross talk contribution into the adjacent mass channel measured prior to launch was identical to that observed in the flight data. Thus errors in the xenon composition due to shifts in the RF are considered negligible, and this further validates use of the intensity corrections derived from the calibration data. The error bars given in Figure 10 are the standard deviation of these independent measurements of isotopic composition. The conclusion is that the xenon isotopic abundances, for at least those isotopes present at > 5% of the total xenon signal, are solar within the experimental error. A programmed sequence of high-resolution mass scans that could have improved the precision on this measurement were not obtained before the failure of the probe at ~ 23 bar.

Consistent isotope ratios for the EC1 and EC2 regions of sufficient precision to allow a comparison between the various solar system sources were not obtained for Kr. In addition to the statistical errors expected from the low count rates at 82, 84, and 86 amu, there appear to be additional systematic errors. In this particular region of the spectrum, there was a larger offset from the peak center in the mass spectrometer tuning than at the higher or lower masses. It is believed that the wide temperature swings between the EC1 and EC2 regions encountered by the GPMS electronics may have further shifted this offset and affected these peak ratios. Additional errors may arise from spectral interference with the minor krypton isotopes from other species.

8. Conclusions

Table 1 gives a summary of these findings. Within the experimental errors described, the ^{36}Ar/^{38}Ar and ^{20}Ne/^{22}Ne ratios at Jupiter appear to be identical to the solar values. Solar ratios of 5.77 $\pm$ 0.08 and 13.81 $\pm$ 0.08 for argon and neon, respectively, are obtained from laboratory measurements of individual lunar

Table 1. Noble Gas Mixing Ratio or Isotope Ratio at Jupiter

Ratio	Value	Notes
Ar/H_2	1.82×10^{-5}	(2.5 ± 0.5) x solar
Kr/H_2	9.3×10^{-9}	(2.7 ± 0.5) x solar
Xe/H_2	8.9×10^{-10}	(2.6 ± 0.5) x solar
$^{36}Ar/^{38}Ar$	$(5.6 + 0.25)$	vs (5.77 ± 0.08) solar [*Pepin et al.*, 1999]
$^{20}Ne/^{22}Ne$	$(13 + 2.0)$	vs (13.81 ± 0.08) solar [*Pepin et al.*, 1999]
^{128}Xe/(total Xe)	0.018 ± 0.094	normalized to 1.0 for xenon isotopes measured
^{129}Xe/(total Xe)	0.285 ± 0.075	
^{130}Xe/(total Xe)	0.038 ± 0.138	
^{131}Xe/(total Xe)	0.203 ± 0.088	
^{132}Xe/(total Xe)	0.290 ± 0.068	
^{134}Xe/(total Xe)	0.091 ± 0.074	
^{136}Xe/(total Xe)	0.076 ± 0.126	

regolith grains [*Pepin, et al.*, 1999]. The Jovian ratio of the minor krypton isotopes to ^{84}Kr could not be established with the accuracy necessary to discriminate between various other planetary sources. The Jovian xenon fractionation line relative to nonradiogenic terrestrial xenon falls near the solar values predicted by *Pepin* [1991]. The mixing ratio of xenon, krypton, and argon relative to H_2 falls in the 2-4 times solar previously established for N, S, and C.

In the paper by *Niemann et al.* [1998], we pointed out that the noble gas abundance data available at that time argued against clathrate hydrates as the carrier phases in the icy grains that delivered these gases to Jupiter. We can sharpen this argument with the results presented here. According to *Lunine and Stevenson* [1985], with C/H at the Jovian value of 3 times solar, we should expect Xe/Ar > 9 times solar if clathrates were the carriers. Instead, we find Xe/Ar is equal to the solar value, strengthening the idea that the gases were simply trapped in amorphous ice.

This conclusion and the solar values for the noble gas isotopes that we have found are consistent with our earlier deduction that the icy planetesimals that brought the heavy elements to Jupiter were formed at temperatures below ~30K [*Owen et al.*, 1999]. This is much colder than the temperatures commonly associated with the formation of Oort cloud comets in the solar nebula. It will thus be extremely interesting to measure the complete range of noble gas abundances and isotopic ratios directly in comets. This should become possible in the future with rendezvous missions to comets.

Acknowledgments. This work was greatly facilitated by analysis and laboratory data acquisition software developed by Willis Wilson and Eric Raaen This work was supported in part by a grant from NASA's Planetary Atmospheres program.

References

Anders, E., and N. Grevesse, Abundances of the elements: Meteoritic and solar, *Geochim Cosmochim Acta, 53*, 197-214, 1989.

Bar-Nun, A., I. Kleinfeld, and E. Kochavi, Trapping of gas mixtures by amorphous water ice, *Phys. Rev. B., 38*, 7749-7754, 1988

Folkner, W M , R Woo, and S Nandi, Ammonia abundance in Jupiter's atmosphere derived from attenuation of the Galileo probe's radio signal, *J Geophys Res 103*, 22,847-22,856, 1998

Krankowsky, D , C , The composition of comets, In *Comets in the Post-Halley Era* (edited by R. L Newburn Jr., M. Neugebauer, and J Rahe) pp 855-878, Kluwer, Norwell, Mass., 1991.

Lunine, J., and D.J Stevenson, Thermodynamics of clathrate hydrate at low and high pressures with application to the outer solar system. *Astrophys J Suppl., Ser., 58*, 493-531, 1985

Mahaffy, P R., T.M Donahue, S.K. Atreya, T.C. Owen, and H.B. Niemann, Galileo Probe measurements of D/H and $^3He/^4He$ in Jupiter's atmosphere, in *ISSI Space Sci Ser*, vol. 4, *Primordial Nuclei and Their Galactic Evolution* edited by R. von Steiger et al., pp. 251-263, Kluwer Acad., Norwell, Mass., 1998.

Mizuno, H , Formation of the giant planets, *Prog. Theor. Phys. 64*, 544-557, 1980.

Niemann, H. B., D.N. Harpold, S.K. Atreya, G.R. Carignan, D.M. Hunten, and T.C Owen, Galileo Probe Mass Spectrometer experiment, *Space Sci. Rev., 60*, 111-142, 1992.

Niemann, H.B., S.K. Atreya, G.R.Carignan, T.M. Donahue, J.A. Haberman, D.N. Harpold, R.E. Hartle, D.M. Hunten, W.T. Kasprzak, P.R. Mahaffy, T.C. Owen, N.W. Spencer, and S.H. Way, The Galileo Probe Mass Spectrometer: composition of Jupiter's atmosphere, *Science*, **272**, 846-849, 1996.

Niemann, H. B., S. K. Atreya, G. R Carignan, T. M. Donahue, J. A. Haberman, D. N Harpold, R. E. Hartle, D. M. Hunten, W. T. Kasprzak, P. R. Mahaffy, T. C. Owen, and S. H. Way, The composition of the Jovian atmosphere as determined by the Galileo probe mass spectrometer *J. Geophys. Res., 103*, 22831-22846, 1998.

Owen, T., P.R Mahaffy, H.B. Niemann, S. Atreya, A. Bar-Nun, T. Donahue, and I. de Pater, A low-temperature origin for the planetesimals that formed Jupiter, *Nature 402*, 269, 1999.

Owen, T. and A. Bar-Nun, Comets, impacts and atmospheres, *Icarus, 116*, 215-226, 1995.

Pepin, R O., On the origin and early evolution of terrestrial planed atmospheres and meteoritic volatiles, *Icarus, 92*, 2-79,1991.

Pepin, R.O , R.H. Becker, and D.J. Schluter, Irradiation records in regolith materials. I: Isotopic compositions of solar-wind neon and argon in single lunar mineral grains, *Geochim. et Cosmochim. Acta, 63*, 2145-2162, 1999

Pollack, J.B., P. Bodenheimer, Theories of the origin and evolution of the Giant Planets in *Origin and Evolution of Planetary and Satellite Atmospheres*, edited by S.K. Atreya, J.B. Pollack, and M.S. Matthews, pp. 564-604, Univ.Ariz. Press, Tucson, 1989.

Pollack, J.B., M. Podolak, P. Bodenheimer, and B. Christofferson, Planetesimal dissolution in the envelopes of the forming, giant planets, *Icarus 67*, 409-443, 1986.

Wyckoff, S , S C Tegler, and L. Engel, Nitrogen abundance in Comet Halley, *Astropyhs. J., 367*, 641-648, 1991.

A. Alpert, Department of Planetary Sciences, University of Arizona, Tucson, AZ 85721

S K Atreya and T. M. Donahue, Department of Atmospheric, Oceanic and Space Sciences, University of Michigan, 2455 Hayward Street, Ann Arbor, MI 48109.

J. Demick, Department of Engineering, Auburn University, Auburn, AL 36830

D. N. Harpold, P. R. Mahaffy, and H. B. Niemann, Code 915, Laboratory for Atmospheres, (paul.r.mahaffy@gsfc.nasa.gov) Goddard Space Flight Center, Greenbelt, MD 20771

T. C. Owen, Institute for Astronomy, University of Hawaii, 2680 Woodlawn Drive, Honolulu, HI 96822.

(Received December 3, 1999; revised March 14, 2000, accepted March 29, 2000)